

The optical conductivity of half-filled Hubbard ladders

J. Hopkinson and K. Le Hur

Département de Physique and CERPEMA, Université de Sherbrooke, Sherbrooke, Québec, Canada, J1K 2R1

(Dated: October 30, 2018)

We investigate the optical conductivity of half-filled N -leg Hubbard ladders far into the “deconfinement” limit (i.e., weak Hubbard interaction and relatively strong interchain hopping). The N -leg Hubbard ladder is equivalent to an N -band model with velocities obeying $v_1 = v_N < v_2 = v_{N-1} < \dots$. When N is not too large ($N = 3, 4, \dots$), the band pairs $(i, N + 1 - i)$ successively flow to the D-Mott state leading to a cascade of charge and spin gaps [U. Ledermann, K. Le Hur, and T. M. Rice, Phys. Rev. B **62**, 16383 (2000)], and to the progressive closing of the two-dimensional (2D) Fermi surface (FS). The optical conductivity at finite temperatures can then exhibit coexistence between a prominent Drude peak and a high-frequency preformed pair continuum, split by sharp excitonic peaks arising due to an approximate $SO(8)$ symmetry. For very large (but finite) N , all neighboring bands interact on the 2D FS, leading to a low-temperature 2D Mott crossover accompanied by a Spin Density Wave (SDW) instability (similar to the 2D case). In this limit the optical conductivity exhibits a unique charge gap -excitations above the gap being bound hole-pairs- and that the exciton features vanish. These results could help to explain the optical conductivity of 2D systems at and close to half-filling, an example of which is the pseudogap phase of high- T_c cuprates.

PACS numbers: 71.10.Pm;71.30.+h;72.10.-d

I. INTRODUCTION

Understanding the nature of the interplay between *strong* interactions (generally emerging at the stoichiometric electron density due to the possibility of umklapp scattering) and *dimensionality* is an important open matter relevant to a large class of materials including the cuprate superconductors and quasi one-dimensional (1D) organic conductors. The latter can be viewed as possible realizations of coupled one-dimensional Hubbard chains at half-filling where electrons can hop from chain to chain (although the quarter-filled chains are weakly dimerized allowing half-filled umklapps, there is increasing evidence that quarter-filled umklapp scattering dominates the physics)¹. In particular, the Fabre salt family $(TMTTF)_2X$ ($X = ClO_4, Br$ and PF_6) displays insulating behavior at ambient pressure up to quite high temperatures. This reflects the presence of strong umklapp scattering (interaction, U) along the chains due to the commensurate filling resulting in a 1D Mott transition; essentially one has virtually uncoupled insulating chains (**confinement**)^{2,3,4}.

By contrast, substitution of Se for S to create the Bechgaard salt $(TMTSF)_2PF_6$, increases the hopping between chains (t_{\perp}) or alternately decreases the dimerization sufficiently to delocalize particles in the transverse direction (inducing **deconfinement**). The system thus exhibits a crossover to a regime of metallic planes (as t_{\perp} scales to strong coupling faster than U). Experimentally this dimensional crossover takes place around $100K$ in $(TMTSF)_2PF_6$; This is manifested by a change from T (single-chain Luttinger liquid) to T^2 (Fermi liquid) behavior of the dc transport along the chain axis⁵. However, such compounds are located quite close to the confinement transition such that the optical conductivity of $(TMTSF)_2PF_6$ exhibits many features in common with

the single-chain Mott insulator⁶ $(TMTTF)_2PF_6$. Indeed, only 1% of the spectral weight⁶ contributes to the dc (Fermi liquid) transport. Some theoretical attempts to reproduce this result (which bears a superficial resemblance to our half-filled chains for small N (see Fig. 1)), have been performed recently using Dynamical Mean Field Theory (DMFT)⁷ and RPA⁸.

Here, we are additionally motivated to tackle the physics of 2D Cu-O planes of cuprate materials at and close to half-filling where Mott physics (“Mottness”⁹) is also ubiquitous¹⁰; We systematically investigate the behavior of the optical conductivity for half-filled N -leg Hubbard ladders (=coupled chains) *far* into the “deconfinement” regime (the bare transverse hopping amplitude is almost equal to the longitudinal hopping amplitude). For weak on-site repulsion, we can make use of our previous band approach for half-filled N -leg Hubbard ladders¹¹. This allows us to properly take into account the renormalization of the different coupling channels (umklapp, Cooper,...) and also to provide a rigorous study of the ground state. The N -leg Hubbard ladder is equivalent to an N -band model where at half-filling the Fermi velocities obey $v_1 = v_N < v_2 = v_{N-1} < \dots$.

For small N ($N = 3, 4, \dots$), this model results in a cascade of energy scales¹¹, where band pairs $(i, N + 1 - i)$ successively flow to the D-Mott state which possesses an enlarged $SO(8)$ symmetry; This is reminiscent of the two-leg ladder behavior¹². This leads to a complex behavior of the optical conductivity: a Drude peak and a high-frequency particle-hole continuum coexist, with sharp exciton peaks appearing below the continuum reflecting the underlying $SO(8)$ symmetry.

By increasing considerably the number of chains, “four-band” couplings (Fig. 2) become relevant on the 2D Fermi surface. At sufficiently low temperatures, a 2D insulating transition with strongly enhanced SDW corre-

lations arises¹³. *The low-energy physics already converges to that of the purely 2D Hubbard model*^{10,14}. We rigorously establish that charge excitations above the Mott gap consist of bound hole-pairs (preformed pairs) and that the excitonic peaks cannot survive in this limit. This could be relevant to an understanding of optical conductivity measurements on the high- T_c cuprates at and close to half-filling¹⁵; Indeed, umklapp scattering should not be ignored in the underdoped regime of the cuprates—features seen above $\sim 2eV$ and the transfer of spectral weight as a function of doping or temperature (T) reflect this importance.

II. THE MODEL

Our starting point is the N-leg Hubbard ladder model,

$$H_{Kin} = -t \sum_{x,i,s} d_{is}^\dagger(x+a)d_{is}(x) + \text{h.c.} \\ -t_\perp \sum_{x,i,s} d_{i+1s}^\dagger(x)d_{is}(x) + \text{h.c.}; \quad (1)$$

t and t_\perp denote the hopping matrix elements along and perpendicular to the chains, a is a lattice step, and $d_{is}(x)$ annihilates an electron with spin s on chain i at the rung x . The interaction term reads

$$H_{Int} = U \sum_{i,x} d_{i\uparrow}^\dagger(x)d_{i\uparrow}(x)d_{i\downarrow}^\dagger(x)d_{i\downarrow}(x), \quad (2)$$

where U is the on-site Hubbard repulsion. Again, here we are investigating the perfect “deconfinement” regime which implies that the perpendicular hopping t_\perp is sufficiently large to deconfine *all* the electrons in the transverse direction. More precisely, below, we consider the weak-interaction limit $0 < U \ll (t, t_\perp)$ where tractable (and rigorous) calculations are indeed possible¹¹. It is convenient to use the *band picture* where the kinetic part simply takes a diagonal form:

$$H_{Kin} = \sum_{i=1\dots N,s} \int dk \epsilon_i(k) \Psi_{is}^\dagger(k) \Psi_{is}(k); \quad (3)$$

Ψ_{is}^\dagger and Ψ_{is} are the creation and annihilation operators for the band i and

$$\epsilon_i(k) = -2t \cos(ka) - 2t_\perp \cos(k_\perp a). \quad (4)$$

The transverse (Fermi) momenta here simply obey $k_\perp = \pm\pi i/(a(N+1))$ and at half-filling the longitudinal momenta are exactly determined by $\epsilon_i(k_{Fi}) = 0$. The resulting Fermi velocities $v_i = \frac{2ta}{\hbar} \sin(k_{Fi}a)$ then take the form

$$v_i = v_{\bar{i}} = \frac{2a}{\hbar} \sqrt{t^2 - \{t_\perp \cos[\pi i/(N+1)]\}^2}, \quad (5)$$

where $\bar{i} = N+1-i$. The transformation from chain to band (with open boundary conditions) reads¹⁶:

$$d_{is} = \sum_m \sqrt{\frac{2}{N+1}} \sin\left(\frac{\pi m i}{N+1}\right) \Psi_{ms}. \quad (6)$$

For more details on the method at half-filling, see Ref. 11.

Two different limits arise. When N is *not too large*, careful investigation of the coupled Renormalization Group equations (RGEs) of the interacting N-band problem yields a hierarchy of energy scales, $T_i \sim te^{-\alpha v_i \hbar/(aU)}$ (α is a constant parameter of the order of 1), $T_1 > T_2 > \dots > T_r$ —for N even $r = N/2$ and for N odd $r = (N+1)/2$, where band pairs (i, \bar{i}) decouple from all other bands and freeze out. This decoupling, due to band pair umklapp terms satisfying $(k_{Fi} + k_{F\bar{i}}) = \pi/a$, opens both a charge and spin gap. The effective *single-particle* gaps are approximately given by $\Delta_j = T_j$. More precisely, the couplings of the band pairs (i, \bar{i}) scale towards the two-leg ladder fixed point with SO(8) symmetry¹². To compute the optical conductivity in this limit, it will be crucial to exploit this enlarged symmetry. When N becomes *large* (but finite), our method is still rigorous provided the energy difference between two neighboring bands is much larger than the largest relevant energy gap in the problem, i.e., $te^{-t/U}$. This imposes the condition¹⁶ $U < t/\ln N, t_\perp/\ln N$. Here, coupling between neighboring bands leads to a 2D-like SDW instability (crossover)—opening a Mott gap—at the temperature¹³:

$$T_{sdw} \sim te^{-\frac{N}{U \sum_{i=1}^{N/2} \frac{a\hbar}{v_i}}}. \quad (7)$$

Since we are considering relatively large bare values of t_\perp (i.e., perfect nesting on the 2D FS), the resulting charge gap $\Delta \sim T_{sdw}$ is homogeneous on the 2D Fermi surface. When substantially decreasing t_\perp (approaching the confinement transition), we expect that the physics would have a larger dependence on the transverse momenta^{8,17} k_\perp . Finally, ground-state charge properties still resemble those of the small-N (two-band) limit.

III. SMALL N: MAPPING TO SO(8)

For small N, the low-energy Hamiltonian is then the sum of $N/2$ [(N-1)/2 for N odd] two-leg ladder Hamiltonians $H_{i,\bar{i}}$ corresponding to the band pairs (i, \bar{i}) plus the Hamiltonian of a single chain for N odd H_s ¹¹.

Let us consider the case $N = 3$ for simplicity. Here, the relevant couplings of bands 1 and 3 flow towards the universal ratios of the two-leg ladder, and therefore the low-energy Hamiltonian $H_{1,3}$ can be rewritten in terms of an SO(8) Gross-Neveu model (as shown previously by Lin, Balents, and Fisher for the two-band model¹²)

$$H_{1,3} = \int dx \left\{ -iv_1 \sum_{a=1}^4 \Psi_a^\dagger \tau^z \partial_x \Psi_a - g \left(\sum_{a=1}^4 \Psi_a^\dagger \tau^y \Psi_a \right)^2 \right\}. \quad (8)$$

We have implicitly introduced operators $\Psi_{R/La}$ for right and left moving fermions and the Pauli matrices τ^i act on right and left sectors. Even though the four Dirac fermions above are related to the *charge* and *spin* degrees of the two bands, they cannot be simply identified as the original (real) fermions on each band; for a complete map,

see Ref. 12. The low-energy physics emerging from bands 1 and 3 depends on a single coupling g (whose bare value is of the order of U). It is straightforward to show that the interacting part of $H_{1,3}$ both opens a charge and spin gap equal to $2\Delta_1 = 4g < \Psi_a^\dagger \tau^y \Psi_a > \sim 2T_1$. The ground state corresponds to the ‘‘D-Mott state’’: a Mott insulator having short-range pairing correlations with approxi-

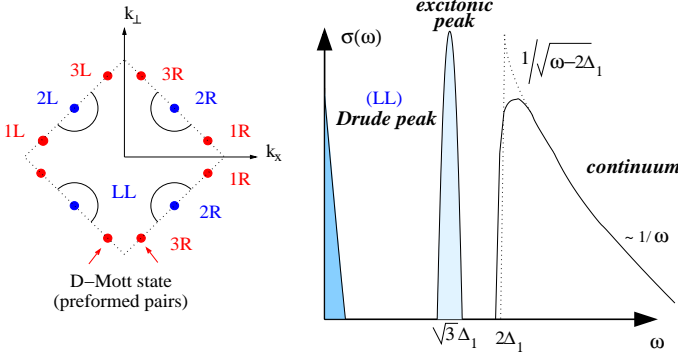


FIG. 1: Optical conductivity of the three-band model for $T_2 \ll T \ll T_1$. The Fermi surface (FS) (drawn for $t_\perp = t$) exhibits a blatant truncation, meaning that bands 1 and 3 form the D-Mott state opening a gap whereas the band 2 is still metallic (and described by a Luttinger theory). The optical conductivity then exhibits a Drude peak (due to band 2), a high-energy continuum (treated here at the mean field level) above the charge gap $2\Delta_1$ and a sharp exciton peak due to the $SO(8)$ symmetry of the D-Mott state.

-mate d-wave symmetry¹². Additionally, fluctuations of the gap around its vacuum value can generate *attractive* interactions between the fermions Ψ_a leading to the formation of *excitons*, whose mass satisfies $M_1 = \sqrt{3}\Delta_1$ (i.e. is smaller than the charge gap of the (localized) preformed-pair continuum¹²). Unlike the single-chain¹⁸, here excitons already appear for purely on-site repulsion.

Band 2 is described by a single chain at half-filling ($\mu = 0$), which is embodied by gapless spinons (spin-1/2 excitations) and the following charge Hamiltonian:

$$H_s^\rho = \int dx \left\{ \frac{u_\rho}{2} \left[\frac{1}{K_\rho} (\partial_x \Phi_\rho)^2 + K_\rho (\partial_x \Theta_\rho)^2 \right] - \frac{g_\rho}{(\pi a)^2} \cos(\sqrt{8\pi} \Phi_\rho) - \mu \partial_x \Phi_\rho \right\}; \quad (9)$$

$\partial_x \Phi_\rho$ describes charge density fluctuations and $\partial_x \Theta_\rho$ current excitations. g_ρ is of the order of U and u_ρ is almost equal to v_2 . It is immediate to check that H_2 induces a charge gap $2\Delta_2 \sim 2T_2 < 2T_1$. Let us now compute the optical conductivity of the three-leg ladder.

Using formula (6), the electrical current can be written in the chain basis as:

$$\begin{aligned} J(x) &= \frac{e}{2i\sqrt{\pi}} \sum_{is} \frac{1}{\delta t_i} (d_{is}^\dagger(x+a)d_{is}(x) - d_{is}^\dagger(x)d_{is}(x+a)) \\ &= \frac{e}{2i\sqrt{\pi}} \left(\frac{v_{D1}}{a} (\Psi_{2s}^\dagger(x+a)\Psi_{2s}(x) - \Psi_{2s}^\dagger(x)\Psi_{2s}(x+a)) \right. \end{aligned}$$

$$\begin{aligned} &+ \frac{v_{D1} + v_{D2}}{2a} (\Psi_{1s}^\dagger(x+a)\Psi_{1s}(x) - \Psi_{1s}^\dagger(x)\Psi_{1s}(x+a)) \\ &+ \Psi_{3s}^\dagger(x+a)\Psi_{3s}(x) - \Psi_{3s}^\dagger(x)\Psi_{3s}(x+a) \\ &+ \frac{v_{D1} - v_{D2}}{2a} (\Psi_{1s}^\dagger(x+a)\Psi_{3s}(x) + \Psi_{3s}^\dagger(x+a)\Psi_{1s}(x) \\ &\left. - \Psi_{1s}^\dagger(x)\Psi_{3s}(x+a) - \Psi_{3s}^\dagger(x)\Psi_{1s}(x+a) \right), \quad (10) \end{aligned}$$

where we have summed up over the contribution coming from each spin s and each leg $i = 1, 2, 3$ of the ladder. Symmetry of the ladder dictates that the drift velocity (v_{D1}) in chains 1 and 3 be equal, although not necessarily the same as in chain 2 (v_{D2}), and the time interval for a hop of one lattice spacing, a , has been taken as $\delta t_i = \frac{a}{v_{D_i}}$. Note that were these velocities equal, the coefficients of the first two terms in the band basis would be identical while the third would disappear leaving a straight sum over bands. Indeed, the last term is found to contain an oscillatory contribution in x , which, when inserted into Eq. 12 vanishes. In linear response, the optical conductivity (at $k = 0$) takes the standard form

$$\Re \sigma(\omega) = \Im m \left(\frac{\Pi(\omega)}{\omega} \right), \quad (11)$$

the current-current correlator being

$$\Pi(\omega) = \frac{1}{\hbar} \int dx d\tau e^{i\omega_n \tau} \langle T_\tau J(x, \tau) J(0, 0) \rangle_{\omega_n \rightarrow -i\omega + \delta}. \quad (12)$$

In the three-leg ladder, we find the following current

$$\begin{aligned} J &= \frac{\sqrt{2}}{\pi} e (v_{D1} \partial_x \Theta_\rho + \frac{v_{D1} + v_{D2}}{2} \sqrt{2} \sin(k_{F1} a) \partial_x \Theta_{\rho+}) \\ &= J_{1band} + J_{2band}, \end{aligned} \quad (13)$$

where one can re-express the 2-band contribution in terms of Majorana fields (real chiral fermions $\psi_{R/La} = \eta_{R/L2a-1} + i\eta_{R/L2a}$) as

$$\begin{aligned} J_{2band} &= -\frac{(v_{D1} + v_{D2})e}{\sqrt{2\pi}a} \sin(k_{F1} a) \Psi_1^\dagger \tau^z \Psi_1 \\ &= -\frac{(v_{D1} + v_{D2})ie\sqrt{2}}{\sqrt{\pi}a} \sin(k_{F1} a) (\eta_{R1}\eta_{R2} - \eta_{L1}\eta_{L2}). \end{aligned} \quad (14)$$

Using Eq. 12, the contribution of these terms to the conductivity is,

$$\begin{aligned} \Re \sigma_{2band}(\omega) &= \frac{-e^2 (v_{D1} + v_{D2})^2 \sin^2(k_{F1} a)}{\pi a^2 \hbar \omega} \Im m \left\{ \int dx \right. \\ &\left. \int d\tau e^{i\omega \tau} \sum_{P=R,L} \langle T_\tau \eta_{P1} \eta_{P2}(x, \tau) \eta_{P1} \eta_{P2}(0, 0) \rangle \right\}. \end{aligned} \quad (15)$$

As pointed out in Ref. 12, since the two-band model is equivalent to the $SO(8)$ Gross-Neveu model whose excitation spectrum is known, below the D-Mott gap mass M_1 bound-states of charge $\pm 2e$ fundamental fermions can form. The latter factor of Eq. 15 bears resemblance to

the ($\vec{k} = 0$) Green's function of a localized particle of mass M_1 , so that

$$\begin{aligned} & - \int dx \int d\tau e^{i0x} e^{i\omega_n \tau} \langle T_\tau \eta_1 \eta_2(x, \tau) (\eta_1 \eta_2(0, 0)) \rangle > \\ & \approx - \int dx \int d\tau e^{i0x} e^{i\omega_n \tau} A e^{-\frac{|x|}{\xi}} e^{-\frac{M_1 \tau}{\hbar}} \\ & \approx \frac{A(\xi - \xi e^{-\frac{L}{\xi}})}{i\omega_n - \frac{M_1}{\hbar}}, \end{aligned} \quad (16)$$

where we have introduced a normalization constant, A, the length of the system, L, which we can take to be infinite relative to the correlation length, ξ as we have power law correlations in this system. This means that for $\omega < 2\Delta_1$, the 2-band contribution to the optical conductivity at T=0 should be

$$\Re \sigma_{2band}(\omega) = \frac{2e^2(v_{D1} + v_{D2})^2 A \xi \sin^2(k_{F1}a)}{a^2 \hbar \omega} \delta(\omega - M_1). \quad (17)$$

As in principle there is only one velocity scale in the (massive) SO(8) Gross-Neveu model, v_1 , one might expect to find $(v_{D1} + v_{D2}) \propto v_1$. However, one might expect the opening of this gap to strongly renormalize v_1 .

An interesting situation emerges when the Fermi surface is partially **truncated**, i.e., when $T_2 \ll T \ll T_1$: Band 2 is still *metallic* whereas bands 1 and 3 already form a D-Mott *insulating* state. In fact, the umklapp term $-\frac{g_\rho}{(\pi a)^2} \cos(\sqrt{8}\pi\Phi_\rho)$ is still small, because its renormalization has been (completely) cutoff by thermal effects. Band 2 then behaves as a single-chain Luttinger liquid which produces a prominent Drude peak of height $\sim 2e^2 v_{D1}/\hbar \sim 2e^2 u_\rho K_\rho/\hbar$ at $\omega = 0$; from this we see that $v_{D1} = v_2$, the Fermi energy of the second band. Moreover, following Ref. 12, the current operator $\Psi_1^\dagger \tau^z \Psi_1$ clearly excites the mass $\sqrt{3}\Delta_1$ excitons, as well as higher energy continuum scattering states (preformed pairs) with energy above $2\Delta_1$. For clarity's sake, results have been summarized in Fig. 1. At very high-frequency, we approximately recover the behavior¹⁹ of a single-chain at half-filling, i.e., $\sigma(\omega) \propto \omega^{-1}$ (see Appendix A).

IV. SMALL N: THE EFFECTS OF TEMPERATURE

As mentioned previously, one certainly would expect a non-trivial role to be played by the temperature of the system. While at strictly T=0, one would expect to see a δ -function peak arising from the bound-state excitonic contribution to the optical conductivity, this peak should be thermally broadened. At $T = 0$, a mean field treatment would predict the spectral weight in the high-energy continuum to have a square-root singularity reflecting the van Hove singularity at the bottom of a band¹²; At $T \neq 0$, the scattering time between the fermions Ψ_1 becomes finite and one would expect $\sigma(\omega = 2\Delta_1, T) \approx e^{\Delta_1/T}$ (finite). On the other hand, since the SO(8) Gross-Neveu model is integrable, the optical conductivity for this state can be found exactly in principle, as it consists of the

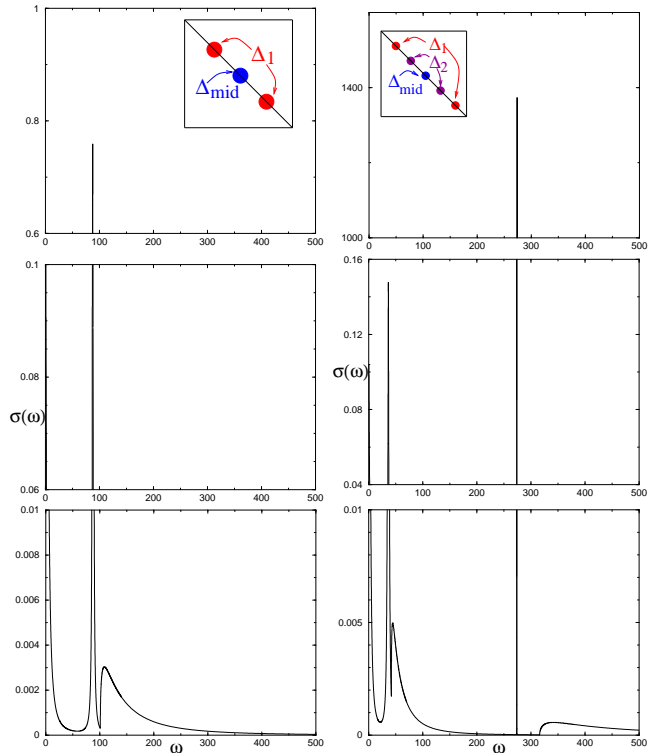


FIG. 2: Optical conductivity for (left) a 3-leg ladder, and (right) a 5-leg ladder. Here we have made the assumptions: $\Delta_{mid} \approx 1meV \approx 10K$ and $t \approx 250meV$, to yield $\frac{v}{t} \approx 0.36$, which defines: (left) $\Delta_1 \approx 50.4K$ and (right) $\Delta_1 \approx 158K$ and $\Delta_2 \approx 20.9K$. Further, temperature has been chosen to reflect the situation of minimal metallic conductivity: (left) $T \approx 20K$ leading to approximately one third of the spectral weight in the Drude-like peak; and (right) $T \approx 15K$ leading to approximately one fifth of the spectral weight in the Drude peak, and temperature broadening effects have been added in a minimal way (see text).

bound-state, 2 particle scattering, and higher particle scattering contributions. Konik and Ludwig²⁰ have calculated the (zero temperature) optical conductivity of the bound-state and the 2-particle scattering contribution of this model to be ($k=0$),

$$\begin{aligned} \Re \sigma_{2band}(\omega) = & A^2 \left(\delta(\omega - \sqrt{3}m) \frac{2\Gamma(1/6)}{9m^2\Gamma(2/3)} \sqrt{\frac{\pi}{3}} \right. \\ & \exp \left[-2 \int_0^\infty \frac{dx}{x} \frac{G_c(x) \sinh^2(x/3)}{\sinh(x)} \right] \\ & + \theta(\omega - 4m^2) \frac{12m^2}{(\omega^2 - 3m^2)^2} \frac{\sqrt{\omega^2 - 4m^2}}{\omega} \exp \left[\int_0^\infty \frac{dx}{x} \right. \\ & \left. \left. \times \frac{G_c(x) (1 - \cosh(x) \cos(\frac{x \cosh^{-1}[\frac{\omega - 2m^2}{2m^2}]}{\pi}))}{\sinh(x)} \right] \right), \end{aligned} \quad (18)$$

where A is an overall constant, $m=\Delta_1$ is the mass of an elementary SO(8) Gross-Neveu particle, and $G_c = \frac{2 \cosh(x/6) - \sinh(x/6) e^{-2x/3}}{\cosh(x/2)}$. In particular, it is useful to no-

tice that the square-root singularity predicted by mean field theory does not survive in the exact calculation. Integration of their result, (assuming higher order scattering processes do not dominate) shows that an astounding 69% of the spectral weight of the two-leg ladder (at zero temperature) is expected to lie within the bound-state. As noted, their results are exact up to the onset of the three-particle continuum, provided one stays at $\omega < \omega_c$, where ω_c is the temperature at which the RG couplings reach their approximate SO(8) coupling ratios. Above this frequency, presumably the chains will begin to behave more and more as individual chains, such that one might expect a crossover from the $\frac{1}{\omega^3}$ high frequency behavior found by Konig and Ludwig²⁰ to an approximate $\frac{1}{\omega}$ as found by Giamarchi¹⁹. The effects of such a crossover have been considered in Appendix A.

In the hopes of making a more simple comparison to experimental curves, we here make the simplest assumptions consistent with a low temperature broadening of the bound-state Gross-Neveu peaks following the treatment by Lin et al¹⁶. There, it was argued that for temperatures $T \ll m$, one could essentially solve the classical Boltzmann equation to obtain a particle density due to thermal excitations of $n \sim \sqrt{mT} e^{-\frac{m}{T}}$. It was further argued that this approximation was self-consistent as the mean free path resulting $l \sim \frac{1}{n}$ would be much greater than the de Broglie wavelength $\lambda \sim \frac{1}{\sqrt{mT}}$, meaning that although the scattering processes themselves were quantum-mechanical, one could think of the particles essentially classically in between these time periods, leading to a time between collisions $\tau \sim \frac{2\pi e^{\frac{m}{T}}}{T}$. Furthermore, they argued that the shape of temperature-broadened bound-state peak should be proportional to this single-particle scattering time, additionally satisfying a scaling ansatz, $\sigma_{peak} \sim \tau \Sigma((\omega - \sqrt{3}m)\tau)$ for $(\omega - \sqrt{3}m) \ll m$.

For our (N-leg) truncated ladders then, the simplest ansatz might be to assume that each δ -function peak is broadened by the lifetime of the particles associated with each successive gap on the Fermi surface; that is, to make the blanket assumption $\tau_i \sim \frac{2\pi e^{\frac{\Delta_i}{T}}}{T}$ and represent the temperature broadened exciton peaks as $\sigma_{peak} \propto \frac{1}{\pi} \frac{\tau_i}{1 + ((\omega - \sqrt{3}\Delta_i)\tau_i)^2}$. In the case of interest, when the temperature is above one of the gaps, one would expect the spectral weight to be distributed about zero, but the breadth of the peak might still be governed by the ratio of the energy scales of the gap relative to the temperature. In such a way, we would expect to simply shift the peak to zero, but effectively keep the same form as the excitonic peak broadenings. To create Fig. 2, we have taken this ansatz in combination with the exact results of Konig and Ludwig²⁰, and the assumption that as the ladder separates into effective 2- and 1-band ladder contributions, the spectral weight in each should be conserved. Additionally, we have input experimental parameters in such a way as might be relevant for a discussion of (TMTSF)₂PF₆, although this leads to an unreasonably high value of $\frac{U}{T} \approx 0.36$ for the validity of

the SO(8) as noted in Appendix A. We note that these results, even if one was well within the validity of the SO(8) symmetry, certainly underestimate the spectral weight in the continuum, as 3- and higher- particle processes have been neglected, in addition to the (unphysical) implicit assumption that there has not been a transfer of spectral weight between the bound-state and continuum as a function of temperature.

None-the-less, the result is a semi-quantitative picture of what one might expect to find in the optical conductivity of the ideal Hubbard ladder system at intermediate temperatures at half-filling (ie. if one could make measurements at frequencies sufficiently small frequencies and temperatures). The percentage of spectral weight in the Drude-peak would be expected to be diminished slightly as one would expect a small Mott contribution close to the relevant energy gap (here 1 meV), but the total spectral weight of this feature when one has only one gap above the temperature scale would be expected to be of the order $\frac{1}{N}$, with a progressive narrowing of the width of this feature as the temperature decreased (as seen for example in (TMTSF)₂PF₆ by Vescoli et al⁶. For the small number of legs where this truncation should occur, one should not be able to achieve such a small percentage of the total weight (1%)⁶ as seen experimentally⁶.

V. LARGE N: ANTIFERROMAGNETIC 4-BAND HOLE PAIRS

Let us now increase considerably the number of chains (we consider the solvable case where the energy difference between band pairs $\sim 1/N$ is larger than the relevant gaps). As long as “4-band” interactions between bands (i, k, \bar{i}, \bar{k}) ($k_{Fi} \rightarrow k_{Fk}, k_{F\bar{i}} \rightarrow k_{F\bar{k}}$) –which stand for 2D-like antiferromagnetic interactions (Fig. 3)– remain *small*, our system is a bunch of (almost) decoupled bands and is still 1D-like. *However, at low-energy, the system clearly behaves as in 2D (See Ref. 13)!* Indeed, two-band and single-band interactions will be dominantly

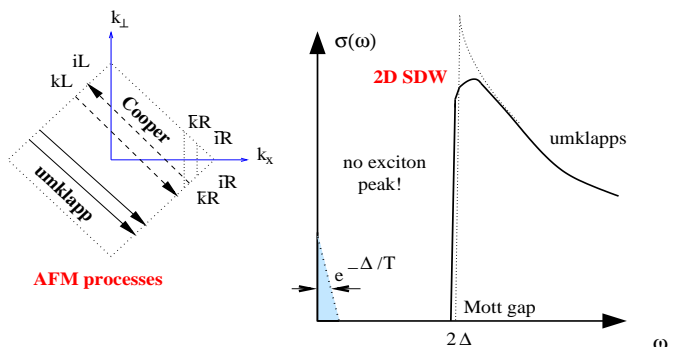


FIG. 3: Optical conductivity of the N-band model for large (but finite) N and $T < T_{sdw}$. 2D antiferromagnetic (AFM) interactions break the SO(8) symmetry (exciton peaks *vanish*); The system flows to a 2D SDW state with a uniform charge gap.

renormalized by the “four-band” interactions: Certain couplings of the band pairs (i, \bar{i}) still grow and tend to approach fixed ratios, however these differ from the small N ratios. Furthermore, for bands k and i which are close together on the FS, as $k \rightarrow i$, the four-band couplings become the same as the corresponding two-band couplings. The one-loop RGEs and theoretical details are given explicitly in Ref. 13. To summarize, all the band pairs now *strongly* interact on the 2D FS, and this leads to a **unique** single-particle (Mott) gap Δ which can be calculated with the asymptotic ratios. Using Eq. (7) for $t_{\perp} \rightarrow t$, we find

$$\Delta \sim T_{sdw} = te^{-\alpha t/(U \ln N)}. \quad (19)$$

The logarithmic corrections come from the fact that $v_1 \approx ta/N$, a precursor of van Hove singularities in 2D. Let us repeat that here $\ln N < t/U$ for the (strict) validity of our calculations. In this limit, it is yet possible to derive the ground-state properties using bosonization¹³.

The pinning of the antisymmetric spin mode between bands i and \bar{i} , $\Phi_{\sigma i \bar{i}-} \approx 0$, produces spinon confinement leaving as physical particles spin-1 magnons. In the symmetric spin sector, only the differences $\Theta_{\sigma i \bar{i}+} - \Theta_{\sigma k \bar{k}+}$ are fixed, such that the total magnon mode(s), given by $\Theta_S = \sqrt{2/N} \sum_{i=1}^{N/2} \Theta_{\sigma i \bar{i}+}$ and $\Phi_S = \sqrt{2/N} \sum_{i=1}^{N/2} \Phi_{\sigma i \bar{i}+}$, remain *gapless*. The spin system behaves increasingly as a 2D SDW in agreement with the strong U limit²¹, and 2D AFM interactions explicitly break the SO(8) symmetry of individual band pairs as it becomes more favorable to pin the mode $\Theta_{\sigma i \bar{i}+} - \Theta_{\sigma k \bar{k}+}$ rather than $\Phi_{\sigma i \bar{i}+}$ ¹³. Finally, 2D AFM interactions do not much affect the ground-state charge properties of band pairs, i.e., as in the small- N limit $\Phi_{\rho i \bar{i}+} \approx 0$ (symmetric charge mode) and $\Theta_{\rho i \bar{i}-} \approx 0$ (antisymmetric superfluid mode).

Let us now discuss the optical conductivity in this large- N limit. First, one can easily show that exciton peaks (that were a blatant signature of the underlying SO(8) symmetry for small- N) cannot persist. Integrating out the spin sector -which now produces antiferromagnetism and then totally *decouples* from the gapped charge sector at low energy- the symmetric charge mode $\Phi_{\rho i \bar{i}+}$ is simply described by a Sine-Gordon model¹³ with $\beta \approx \sqrt{4\pi}$. The spectrum now contains only solitons and anti-solitons (bound hole- (electron) pairs) with dispersion $\epsilon(p) = \sqrt{p^2 + \Delta^2}$. At $\omega \approx 0$ and $T \ll \Delta$, the density of excited carriers evolves like $n \approx e^{-\Delta/T}$, which implies that the Drude peak has an exponentially vanishing weight, reflecting the simultaneous opening of a Mott gap on the whole 2D FS. Finally, at high-frequency, we still find $\sigma(\omega) \propto \omega^{-1}$ (we have almost decoupled bands).

VI. CONCLUSIONS

In closing, we are able to provide a microscopic (low energy) theory for half-filled N -leg Hubbard ladders – even when N is very large– taking into account both the ubiquity of Mott physics and the emergence of promi-

nent antiferromagnetism. At small N , we have demonstrated that it is at least possible within the Hubbard model at half-filling for a system to exhibit metallic behavior over a finite temperature range while maintaining a large Mott contribution, a situation not unlike that seen in (TMTSF)₂PF₆–although the T^2 resistivity encountered in that case has not been recovered here, the relative spectral weight of the Drude feature would be $\mathcal{O}(\frac{1}{N})$ rather than 1%, and the relevant energy scales for this system are well outside the range of validity of our method. At high frequencies one should be able to employ a memory function approach to extract a detailed frequency dependence of the optical conductivity even in regions of moderate coupling. For large N (and $U < t/\ln N, t_{\perp}/\ln N$), the Mott gap opens simultaneously on the 2D FS and, as a precursor of superconductivity, charge excitations resemble hard-core bosons (preformed pairs), whereas spin excitations are gapless magnons (bosons). The optical conductivity is mostly sensitive to the Mott gap opening on the 2D FS (and not to the long-range magnetism) and excitons cannot persist! This seems to be in agreement with results on *half-filled* cuprates¹⁵. When doping, we stress the occurrence of a spin gap and the progressive growth of d-wave phase coherence on the 2D FS. In order to properly discuss the pseudogap phase of cuprates, we must include the effect of a next nearest neighbor hopping²² t' . It is conceivable that such a term might provide a mechanism for the creation of the “mid-gap” states of the doped cuprates^{15,25} (which bear a qualitative resemblance to the two-leg ladder contribution as outlined in Fig. 2), if the effective value of U were to vary substantially around the Fermi surface.

We acknowledge discussions with C. Bourbonnais, R. Duprat, T. Giamarchi, S. Kancharla, A.-M. Tremblay, A. Tsvelik, and financial support by FQRNT and NSERC.

APPENDIX A: GENERIC FEATURES FROM ONE TO THREE CHAINS

A serious problem for this theory is the weakness of U required for the theory to flow to the strong coupling SO(8) fixed point. In particular, this imposes that our gap sizes and hence all of our temperature scales are outrageously low, as the price to pay for the rigor of our treatment. In particular, to actually reach SO(8) within the validity of the 1 loop RG, the half-filled two-leg ladder requires $\frac{U}{t} \leq 2 \times 10^{-6}$, yielding a gap $\sim te^{-500000}$, which for all intents and purposes experimentally might as well be zero. This can be seen from Fig.4, an explicit plot of the ratios of the couplings for the two-leg ladder as a function of the normalized number of steps. For a definition of the couplings of the two and three leg ladder, the reader is referred to Ref.11 and Ref.22. One sees that the curves described by the 1-loop RG equations are universal, although the region of validity decreases as U increases. In the inset, this is seen as a function of the maximal coupling, with ratios expected to reach 1 and 0

if the SO(8) fixed point is reached.

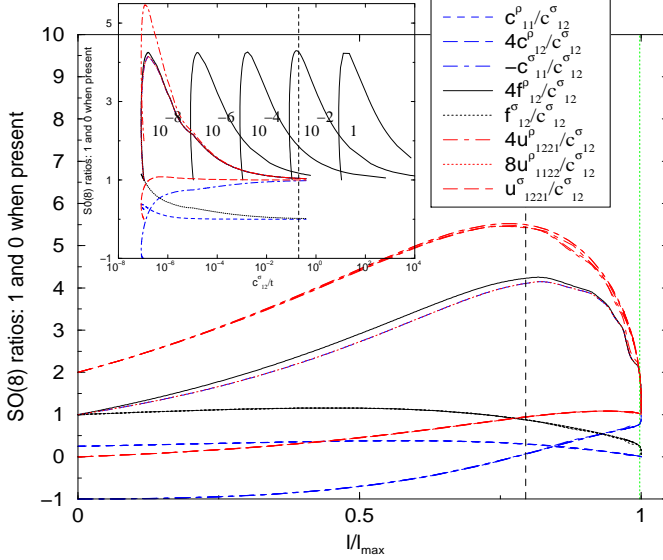


FIG. 4: Validity of the 1-loop RG: (main) Scaling of the RG equations as a function of the number of steps, normalized by the point at which approximate SO(8) symmetry is found (l_{max}). For a definition of the couplings of the two and three leg ladder, the reader is referred to Ref.11 and Ref.22. c_{12}^{ρ} , f_{12}^{ρ} , and u_{1122}^{ρ} have been plotted for $U=10^{-8}$ due to their close proximity, while the remaining curves have been plotted for $t=0.09$, $U=\{10^{-8}, 10^{-6}, 10^{-4}, 10^{-2}, 1\}$ with $l_{max} = (50993400, 508230, 5118.84, 51.7196, 0.51743)$ respectively. The vertical black dashed line delineates the point where the 1-loop RG equations are expected to break down for $U=10^{-2}$, the vertical gray dotted line for $U=10^{-4}$. (inset) The same curves plotted as a function of the ratio of the coupling $\frac{c_{12}^{\sigma}}{c_{12}^{\rho}}$. The vertical dashed line at 0.2, represents the point beyond which the 1-loop RG should not be valid. In principle, these curves could be used to extract the frequency dependence of the umklapp contributions to the two- (and three-) leg ladders as sketched in Fig. 7 and Fig. 8.

Even in the absence of SO(8) symmetry, one clearly can say something about the evolution of the couplings (until the higher order contributions in U become relevant), which means that in principle one could calculate the ω -dependence of the optical conductivity at high frequencies for the two and three leg ladders using a memory function approach²³ akin to Giamarchi's work on the single chain.¹⁹ In this spirit, here we provide a heuristic sketch of such a derivation for the 3-leg ladder, and what one would expect to be the region of its applicability of this perturbative approach. At very high frequencies, one would expect the optical conductivity to break into two components roughly as,

$$\sigma(\omega) = i \frac{2e^2 u_{\rho} K_{\rho}}{\hbar(\omega + M_{1band}(\omega))} + i \frac{4e^2 u_{\rho+} K_{\rho+}}{\hbar(\omega + M_{2band}(\omega))}, \quad (20)$$

where the memory functions, $M_{1band}(\omega)$ and $M_{2band}(\omega)$ can be computed perturbatively in linear response theory

as outlined in Ref. 19 and 24 respectively. In particular one finds that¹⁹ in the limit $\omega \gg T$,

$$M_{1band} = \kappa g_{\rho}^2 \Gamma^2 (1 - 2K_{\rho}) \sin(2\pi K_{\rho}) e^{-i\pi(2K_{\rho}-1)} \omega^{4K_{\rho}-3}, \quad (21)$$

where $\kappa \approx \frac{K_{\rho}}{\pi^3 a^2} \left(\frac{\pi a}{u_{\rho}}\right)^{4K_{\rho}-2}$, and

$$M_{2band} = G_{\chi} \sum_{\chi=1}^4 \left((g_{\chi})^2 \Gamma^2 (1 - (K_{\chi})) \sin(\pi(K_{\chi})) \times e^{-i\pi(K_{\chi}-1)} \omega^{2(K_{\chi}-3)} \right), \quad (22)$$

where $G_{\chi} \approx \frac{K_{\rho+} \sin^2(k_{F_1} a)}{4^3 \pi^3 a^2} \left(\frac{\pi a}{u_{\rho+}}\right)^{2K_{\chi}-2}$

$$g_{\chi} = \begin{cases} 2u_{1331}^{\sigma} & \chi = 1 \\ u_{1331}^{\sigma} + 4u_{1331}^{\rho} & \chi = 2 \\ u_{1331}^{\sigma} - 4u_{1331}^{\rho} & \chi = 3 \\ 16u_{1133}^{\rho} & \chi = 4, \end{cases}$$

and

$$K_{\chi} = \begin{cases} K_{\sigma+} + K_{\rho+} & \chi = 1 \\ K_{\sigma-} + K_{\rho+} & \chi = 2 \\ \frac{1}{K_{\sigma-}} + K_{\rho+} & \chi = 3 \\ \frac{1}{K_{\rho-}} + K_{\rho+} & \chi = 4. \end{cases}$$

For the three-leg ladder, the Luttinger coefficients can be written as, $K_{\rho} = \sqrt{\frac{\pi v_2 - c_{22}^{\rho}}{\pi v_2 + c_{22}^{\rho}}}$, $K_{\rho+} = \sqrt{\frac{\pi v_1 - c_{11}^{\rho} - f_{13}^{\rho}}{\pi v_1 + c_{11}^{\rho} + f_{13}^{\rho}}}$,

$K_{\rho-} = \sqrt{\frac{\pi v_1 - c_{11}^{\rho} + f_{13}^{\rho}}{\pi v_1 + c_{11}^{\rho} - f_{13}^{\rho}}}$, $K_{\sigma+} = \sqrt{\frac{\pi v_1 + \frac{c_{11}^{\sigma}}{4} + \frac{f_{13}^{\sigma}}{4}}{\pi v_1 - \frac{c_{11}^{\sigma}}{4} - \frac{f_{13}^{\sigma}}{4}}}$, and

$K_{\sigma-} = \sqrt{\frac{\pi v_1 + \frac{c_{11}^{\sigma}}{4} - \frac{f_{13}^{\sigma}}{4}}{\pi v_1 - \frac{c_{11}^{\sigma}}{4} + \frac{f_{13}^{\sigma}}{4}}}$. In the high frequency limit, all

couplings, with the exception of u_{1331}^{σ} which vanishes so that one recovers the form of Ref. 24, are of order Ua/\hbar (if one is interested in the exact values, the reader is referred to Table I of Ref. 22), such that the Luttinger coefficients all closely approach 1. Eq. 22 is then the sum of three identical terms. In particular, one finds that $\text{Im}[M(\omega)] \propto U^2 \omega^{2K_{\rho+}-1} \Gamma^2(-K_{\rho+}) \sin^2(\pi K_{\rho+})$. In the opposite limit, the strong coupling SO(8) fixed point corresponds to $0 < g \approx c_{13}^{\rho} \approx 4 f_{13}^{\rho} \approx 4 c_{13}^{\rho} \approx 4 u_{1331}^{\rho} \approx 8 u_{1133}^{\rho} \approx u_{1331}^{\sigma} \approx -c_{11}^{\sigma}$, so that one sees that while K_{ρ} remains close to 1, spin and charge gaps drive $K_{\rho+}, \frac{1}{K_{\rho-}}, K_{\sigma\pm}$ towards 0. If this limit were strictly attainable, then $g_3 = 0$, and Eq. 22 again would become the sum of three identical terms, with a naïve ω^{-3} dependence to $\text{Im}[M(\omega)]$, although it is essential to note both that: the coefficient of such a term would also be highly frequency dependent, and for the small frequencies required for the validity of our theory, $M(\omega)$ would outgrow the perturbative regime required for the memory function's linear response to be valid (despite the smallness of G) a little before this point.

Unlike at the strong coupling point, in the high frequency limit, 3-band umklapp processes are also relevant,

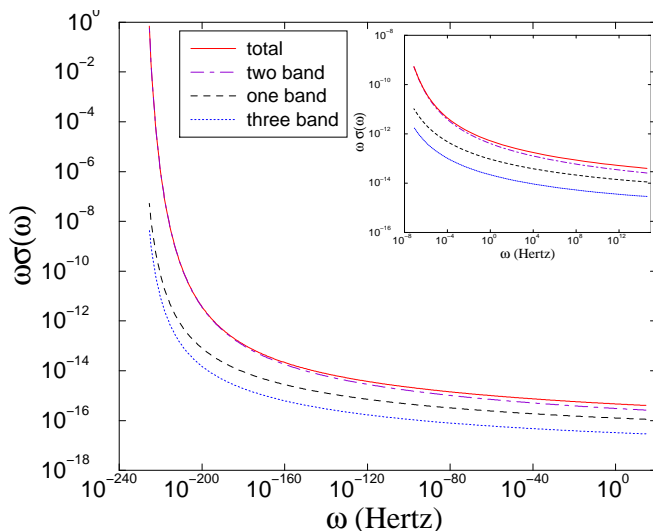


FIG. 5: Using the memory function, we can extract the frequency dependence of the “high frequency” optical conductivity (in S.I. units). Here we have removed the $\frac{1}{\omega}$ dependence for $U/t \approx 0.011$. Notice that one still has substantial frequency dependence in the crossover region and that the magnitude is quickly killed at high frequencies as required to satisfy the optical conductivity sum rules. The asymptotic high frequency dependence is $\sigma(\omega) \sim \omega^{-1.006}$ while as one approaches the Mott gap this changes dramatically, in the small frequency limit here $\sigma(\omega) \sim \omega^{-2.3}$. In the inset, we show $U/t \approx 0.11$, to emphasize the small frequencies are an artifact of the weak coupling limit. The choice $t=0.25$ meV= $4 * 10^{14}$ Hz has been taken, such that we are restricted to $\omega < 2 * 10^{14}$ Hz.

and contribute additional terms to both Eq. 21 and Eq. 22. Letting $g_{\rho} \rightarrow \frac{g_{\nu}}{8}, 2K_{\rho} \rightarrow K_{\nu}, K_{\chi} \rightarrow K_{\nu}$ and $g_{\rho+} \rightarrow \frac{g_{\nu}}{2}$

with,

$$g_{\nu} = \begin{cases} 2u_{1223}^{\sigma} & \nu = 1 \\ u_{1223}^{\sigma} + 4u_{1223}^{\rho} & \nu = 2 \\ u_{1223}^{\sigma} - 4u_{1223}^{\rho} & \nu = 3 \\ 8u_{2213}^{\rho} & \nu = 4, \end{cases}$$

and

$$K_{\nu} = \begin{cases} \frac{1}{4}(K_{\sigma+} + K_{\rho+} + \frac{1}{K_{\rho-}} + \frac{1}{K_{\sigma-}} + 2K_{\rho} + 2K_{\sigma}) & \nu = 1 \\ \frac{1}{4}(K_{\sigma-} + K_{\rho+} + \frac{1}{K_{\rho-}} + \frac{1}{K_{\sigma+}} + 2K_{\rho} + \frac{2}{K_{\sigma}}) & \nu = 2 \\ \frac{1}{4}(K_{\sigma+} + K_{\rho+} + \frac{1}{K_{\rho-}} + \frac{1}{K_{\sigma-}} + 2K_{\rho} + 2K_{\sigma}) & \nu = 3 \\ \frac{1}{4}(K_{\sigma-} + K_{\rho+} + \frac{1}{K_{\rho+}} + \frac{1}{K_{\sigma-}} + 2K_{\rho} + \frac{2}{K_{\rho}}) & \nu = 4. \end{cases}$$

$$\text{Here, } K_{\sigma} = \sqrt{\frac{\pi v_2 + \frac{c_{22}^2}{4}}{\pi v_2 - \frac{c_{22}^2}{4}}}.$$

The real part of the optical conductivity arises as,

$$\Re \sigma_{2band}(\omega) = \frac{4e^2 u_{\rho} K_{\rho} \Im m(M_{2band}(\omega))}{\hbar((\omega + \Re(M_{2band}(\omega)))^2 + (\Im(M_{2band}(\omega)))^2)}, \quad (23)$$

the condition $0.2 \geq \omega^{-1}|M_{2band}(\omega)|$ approximates the region where this formula can be applied. On a 3-leg ladder the region about which our linearization is valid is $\sim \frac{1}{8}$ of the band-width ($4t$). This gives a high energy cut-off on the frequencies we can describe for the 3-leg ladder: $\omega < \frac{t}{2}$ so that one can describe a large range of frequencies (see Fig. 5). This constraint becomes more severe for N large—for $N=16$ one is restricted to $\omega < 0.08t$ —but is expected to still admit a region where the memory function returns $\sigma(\omega) \propto \frac{1}{\omega}$.

¹ For a recent review, C. Bourbonnais in High Magnetic Fields, Applications in Condensed Matter Physics and Spectroscopy, Lecture Notes in Physics, Vol. 595, Ed. C. Berthier, L. P. Levy and G. Martinez, ISBN: 3-540-43979-X, Springer (2003).
² T. Giamarchi, Physica B **230-232**, 975 (1997).
³ D. Controzzi, F. H. L. Essler, and A. M. Tsvelik, Phys. Rev. Lett. **86**, 680 (2001).
⁴ K. Le Hur, Phys. Rev. B **63**, 165110 (2001).
⁵ D. Jerome, Organic Superconductors, From (TMTSF)₂PF₆ to Fullerenes, Chap. 10, p.405, Marcel Dekker Inc. (1994).
⁶ V. Vescoli, L. Degiorgi, W. Henderson, G. Grüner, K. P. Starkey, and L. K. Montgomery, Science **281**, 1181 (1998).
⁷ S. Biermann, A. Georges, A. Lichtenstein, and T. Giamarchi, Phys. Rev. Lett. **87**, 276405 (2001).
⁸ F. H. L. Essler and A. M. Tsvelik, Phys. Rev. B **65**, 115117 (2002).
⁹ T. D. Stanescu and P. Phillips, cond-mat/0301254.
¹⁰ See, e.g., N. Furukawa and T. M. Rice, J. Phys. Cond. Mat. **10** L381 (1998).
¹¹ U. Ledermann, K. Le Hur, and T. M. Rice, Phys. Rev. B

62, 16383 (2000).
¹² H. Lin, L. Balents, and M. Fisher, Phys. Rev. B **58**, 1794 (1998).
¹³ U. Ledermann, Phys. Rev. B **64**, 235102 (2001) (PhD Thesis, Diss. ETH No. 14325); K. Le Hur, unpublished.
¹⁴ On the N-patch model in 2D, see, e.g., D. Zanchi and H. J. Schulz, Europhys. Lett. **44**, 235 (1998).
¹⁵ S. Uchida, T. Ido, H. Takagi, T. Arima, Y. Tokura, and S. Tajima, Phys. Rev. B **43**, 7942 (1991); H. J. A. Molegraaf, C. Presura, D. van der Marel, P. H. Kes, and M. Li, Science **295**, 2239 (2002).
¹⁶ H. Lin, L. Balents, and M. Fisher, Phys. Rev. B **56**, 6569 (1997).
¹⁷ R. Duprat and C. Bourbonnais, Eur. Phys. J. B **21**, 219 (2001).
¹⁸ Z. Shuai, J. L. Brédas, S. K. Pati and S. Ramasesha, Phys. Rev. B **58**, 15329 (1998); N. Tomita and K. Nasu, Phys. Rev. B **63**, 085107 (2001); S. S. Kancharla and C. J. Bolech, Phys. Rev. B **64**, 085119 (2001).
¹⁹ T. Giamarchi, Phys. Rev. B **44**, 2905 (1991).
²⁰ R. Konik and A. W. Ludwig, Phys. Rev. B, **64**, 155112 (2001).

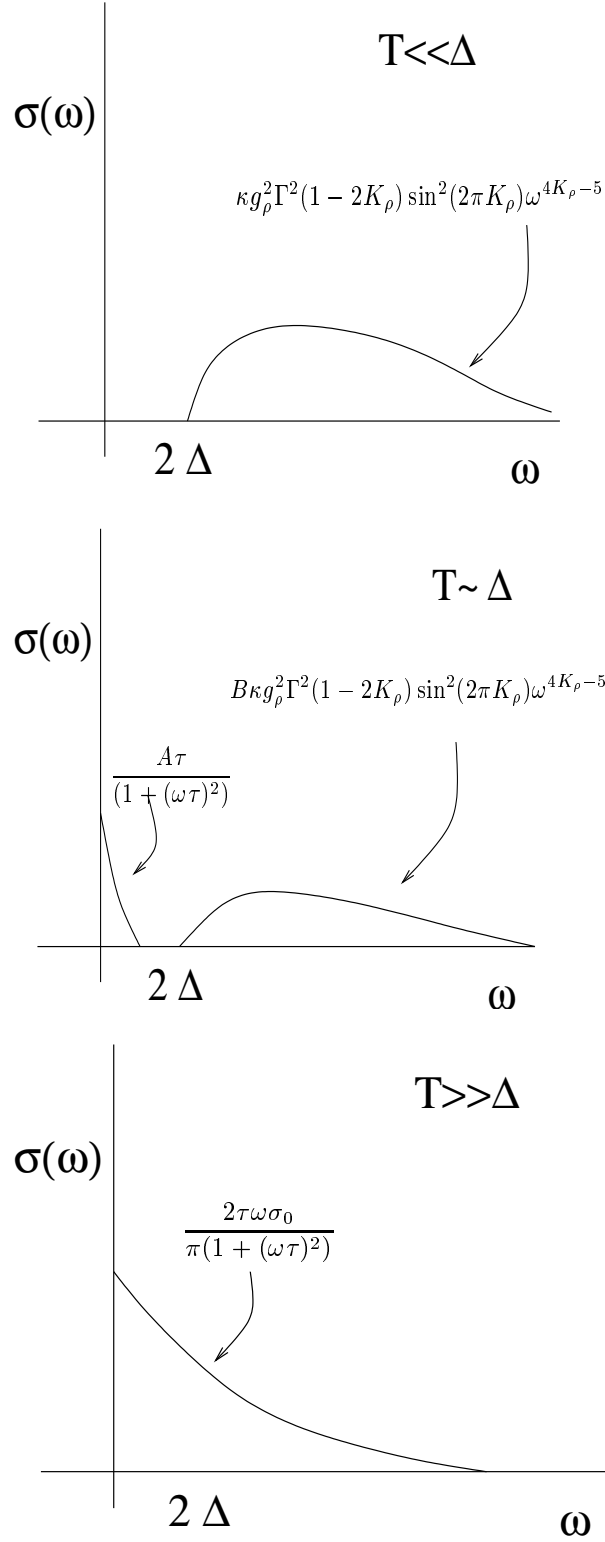


FIG. 6: The effects of temperature on a half-filled single chain system in weak coupling. Here, $\tau = 2\pi e^{\Delta/T}/T$, the $1/\omega$ term is cut off at high frequencies by $K_\rho \rightarrow 1$, where K_ρ and u_ρ are the Luttinger parameters of the single chain, and at intermediate temperatures we would expect to see a partial shift of weight from above the gap to form an $\omega = 0$ Drude peak. A, B and c are constants, g_ρ is the strength of the the umklapp scattering as defined in Eq.9 and 21, while σ_0 is the weight $2 e^2 u_\rho K_\rho / \hbar$.

- ²¹ H. J. Schulz, in *Correlated Fermions and Transport in Mesoscopic Systems*, ed. T. Martin, G. Montambaux, J. Tran Thanh Van (Editions Frontieres, Gif-sur-Yvette, 1996), p. 81.
- ²² J. Hopkinson and K. Le Hur, cond-mat/0308504.
- ²³ W. Götze and P. Wölfe, Phys. Rev. B **6**, 11226 (1972).
- ²⁴ P. Byrne, E. H. Kim and C. Kallin, Phys. Rev. B **66**, 165433 (2002).
- ²⁵ T. Arima, Y. Tokura and S. Uchida, Phys. Rev. B **48**, 6597 (1993).

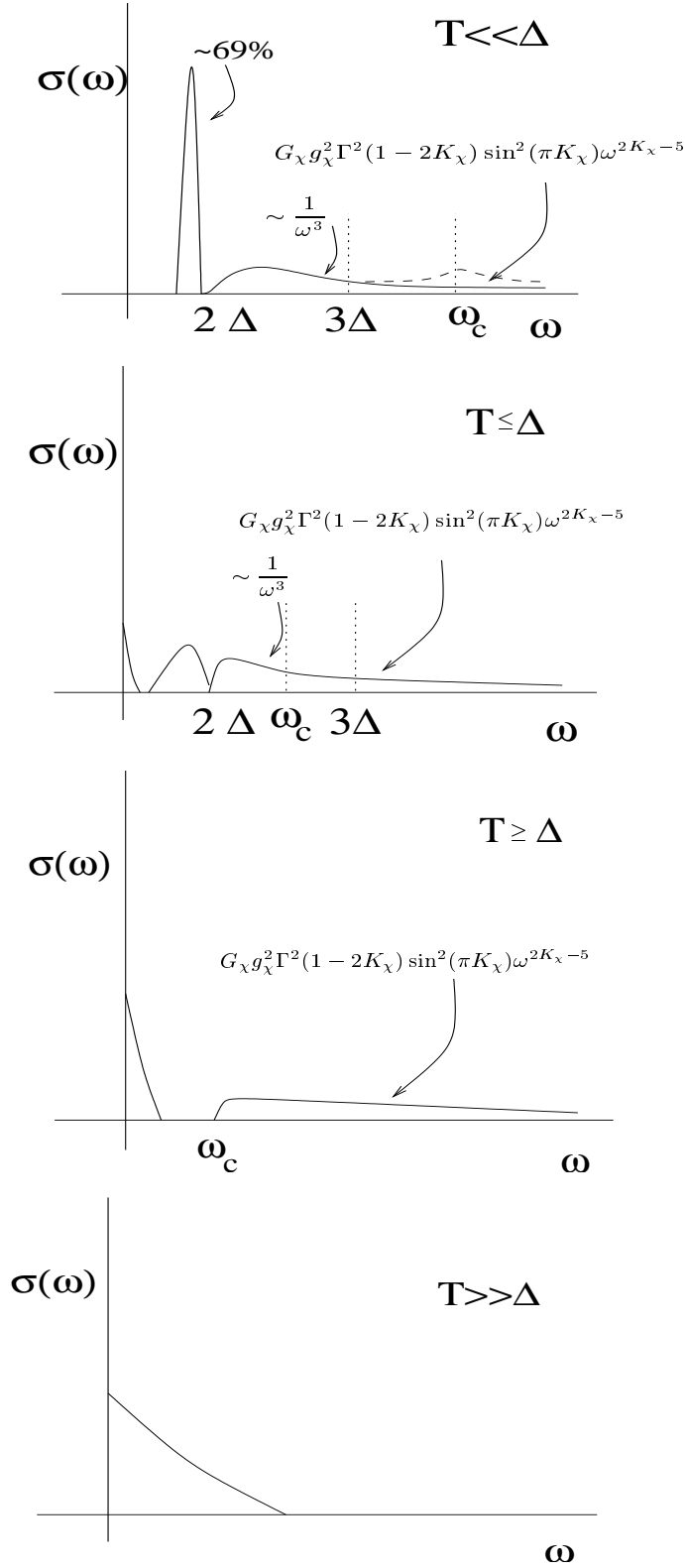


FIG. 7: The evolution of the two-leg ladder optical conductivity as a function of temperature, were the frequencies available experimentally. (top) The majority of the spectral weight would lie in a sharp peak at $\sqrt{3}\Delta$; the onset of 2-particle scattering would be as $\sqrt{\omega - 2\Delta}$; the decrease up to 3Δ would go as ω^{-3} , and cross over to the ω^{-1} form of Giamarchi¹⁹, cut off at high frequencies by the larger of the resistive umklapp scattering terms, when $K_\chi \rightarrow 2$, (where K_χ is defined in the text), such that the optical conductivity sum rule is satisfied. Note that this need not be a simple cross-over of exponents, one might find that this asymptotic behavior arrives higher than the exact low frequency result, leading to a second bump at higher frequencies as outlined with dashed lines. Less weight would be attributed to the exciton as the temperature approached that of the gap, with increasing weight at $\omega = 0$.

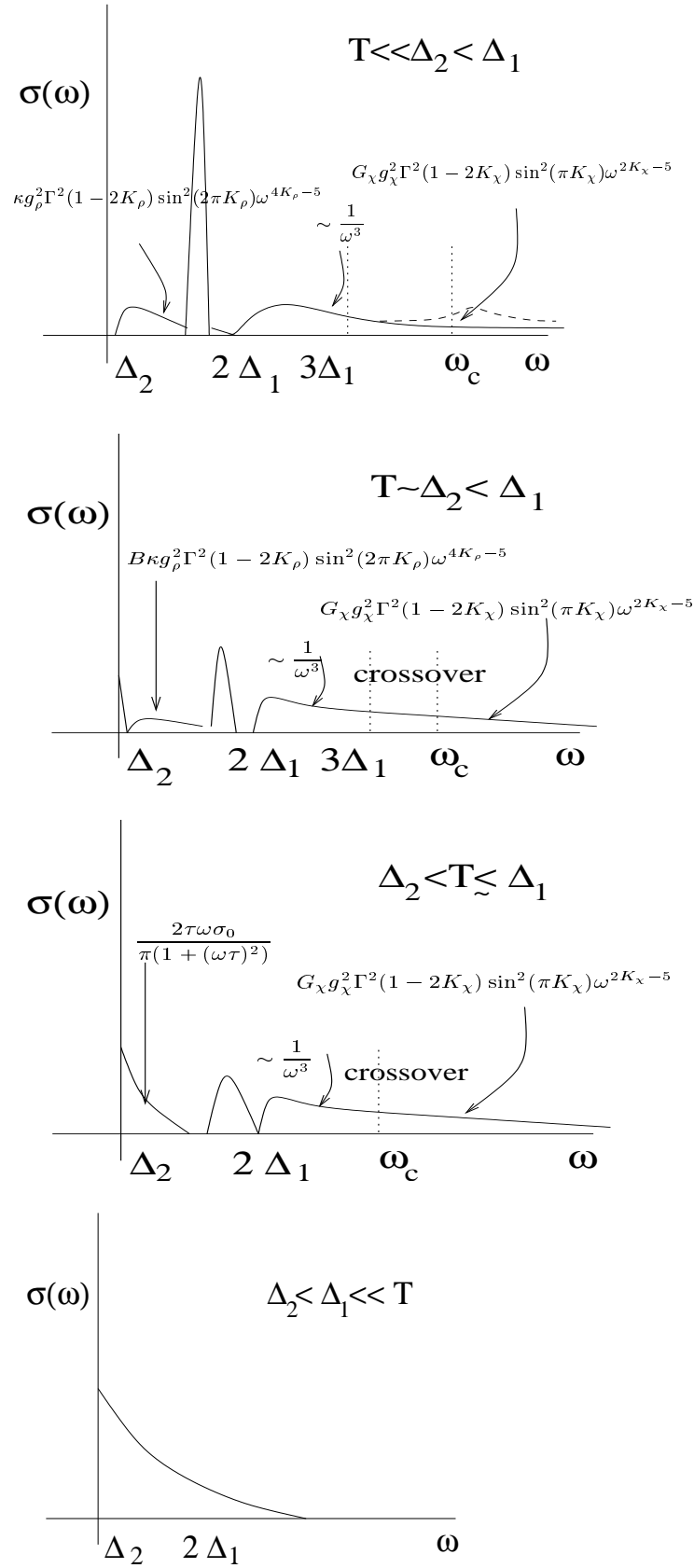


FIG. 8: The evolution of the three-leg ladder as a function of temperature.